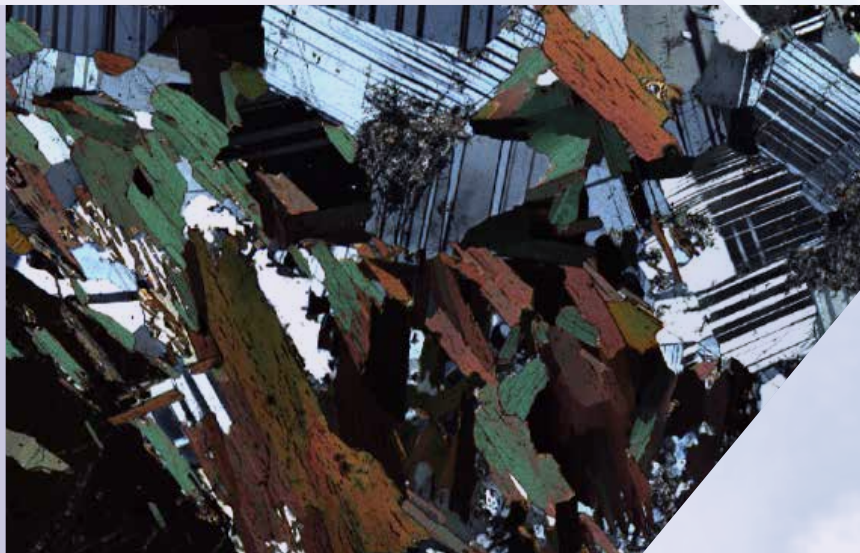
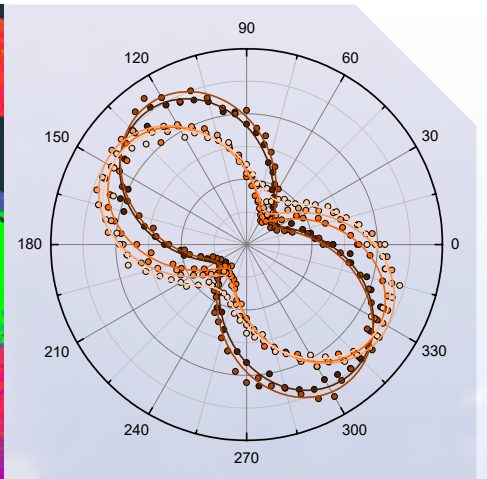
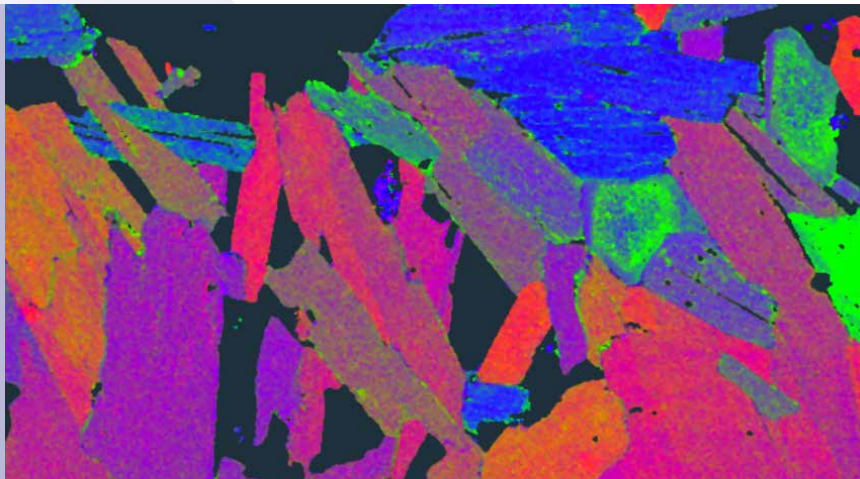


APPLICATION NOTE

Investigation of Biotite with Polarization-resolved White Light and Raman Microscopy



Introduction

Since the invention of polarizers by William Nicol in 1829 and the development of the first polarizing microscope by Giovanni Battista Amici in 1830 [1,2], geosciences and mineralogy have been revolutionized by the ability to analyze rock thin sections between a set of two polarizers with white light illumination. Through the rotation of the two polarizers relative to each other and to the orientation of individual mineral grains, the resulting optical effects allow conclusions to be made about materials' physical properties. Additional polarization-resolved Raman spectroscopy measurements provide detailed insight on the molecular composition and the crystallographic orientations in the rock.

In this investigation we combine both methods and semiquantitative approaches to identify two different formation stages of the mineral biotite based on its geometrical alignment in the sample.

Microscopic setup

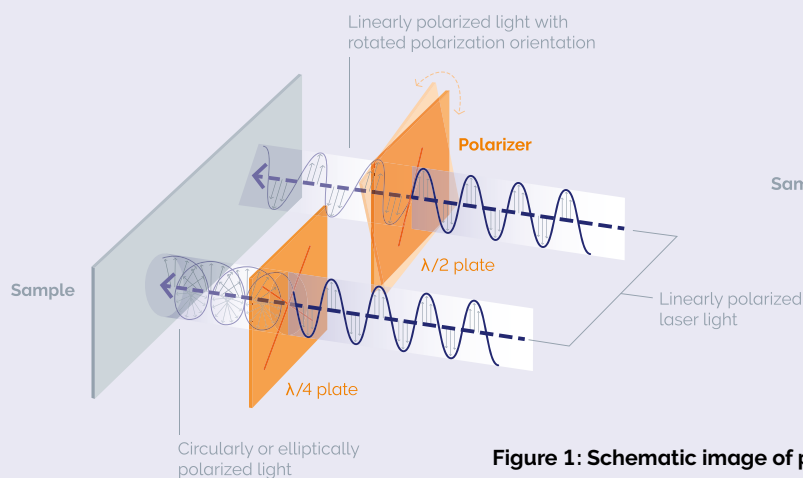
The measurements presented here were performed with an Oxford Instruments WITec alpha300 Raman microscope equipped with integrated polarization modules. For polarized white light imaging, two independent polarization filters were introduced to the optical beam path: the first (polarizer) is positioned behind the unpolarized white light source, the second (analyzer) after the sample in the detection beam path. This setup enabled white light imaging in parallel polarization (parallel-oriented polarizer and analyzer, ||Pol) and cross polarization (orthogonal orientation of polarizer and analyzer, xPol) modes.

For the laser-based polarization-resolved Raman spectroscopic measurements, dedicated polarizer and analyzer modules were used: Here, the polarizer module consists of a freely rotatable half-wave plate that precisely orients the linearly polarized excitation beam's polarization on the sample (Figure 1). The analyzer module in the detection beam path again allows for the selection of a specific linear polarization state of the scattered light to be studied. By rotating the analyzer, the directional emission pattern of a vibrational mode was probed.

Sample

To differentiate geometrically heterogeneous biotite alignments, a sample was chosen in which the relationship between two formation processes (metamorphic crystal alignment vs. magmatic melt penetration) is not obvious from the crosscutting relationship. Figure 2 shows this situation in a stitched white light image of a 40 x 20 mm thin section from the abandoned Griffins Find Gold Mine, Western Australia. Two rock-forming generations could be assumed, as the metamorphic layering fabric of a μm -sized mafic granulite (yellow region: biotite-feldspar-pyroxene) is intersected by a vein of mm-sized mineral grains with different mineralogical paragenesis (red region: quartz-feldspar-biotite-pyroxene). However, it can also be seen that this vein propagates along the lineation and fabric of the metamorphic orientation. This raises the question of whether this difference already existed (e.g. due to irregularities in the parent rock) or a possible melt penetration and recrystallization of the rocks occurred along the pre-developed lineation.

Excitation path



Detection path

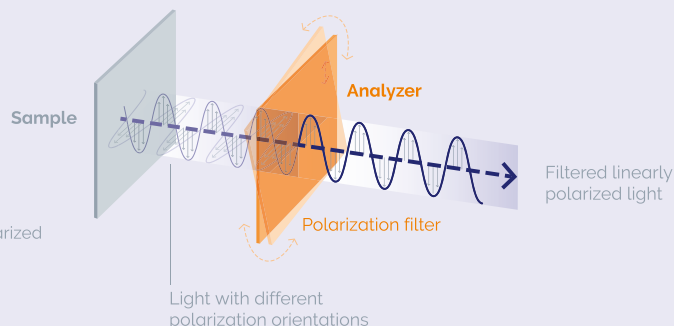


Figure 1: Schematic image of polarization control components.

Excitation path: The coherent, linearly polarized incident light is emitted from a laser with its electric field oscillating perpendicular to the propagation direction. The linear polarization state can be rotated to the desired orientation using a half-wave ($\lambda/2$) plate in the polarizer module. A quarter-wave ($\lambda/4$) plate may be introduced to produce elliptically or circularly polarized light.

Detection path: Using a polarization filter, i.e., the analyzer in the beam path before the detector, the polarization state of the detected light can be selected.

Hypothesis

Single crystals in a metamorphic rock were aligned perpendicular to the direction of pressure over millions of years and then suddenly the rock was fractured and underwent emplacement by melt of magmatic origin. Support for this hypothesis would be found in the detection of highly aligned biotite in the metamorphic areas (pressure-induced solid reactions and deformation) while seeing the full degree of freedom for arbitrary biotite crystallization (cavitation and crystallization from a liquid) in the magmatic areas.

Polarized white light microscopy investigation of biotite crystals

With polarized white light microscopy, optical properties of materials can be visualized to aid in characterizing their composition and structure. The underlying effect – birefringence – is specific for individual materials and is caused by the anisotropy in the crystal lattice, splitting of the polarized light into two beam paths, and different propagation speeds of the electromagnetic waves along different crystal planes. This creates a characteristic phase shift between both waves, which can be represented as interference colors.

Here we show a 25 μm thin rock section in different white light illumination setups to identify the crystal's composition and structure. While reflected and unpolarized transmitted light images (Figures 3A and 3B) show the presence of opaque (ore minerals) and transparent crystals (major rock forming minerals), the coloring visible in the $\parallel\text{Pol}$ illuminated setting (Figure 3C) displays their intrinsic colors and, most importantly, their morphology and formative relationship. The interference colors in the xPol configuration (Figure 3D) indicate which minerals are present and reflect qualitative differences in the crystallographic orientation of their crystal lattices. In combination, the four images reveal mineral phase identities as well as processes of rock formation by connecting optical properties to crystallographic orientations and other crystal properties (i.e. crystal fabrics: habits, cleavages, twinning, inclusions, exsolutions, deformations).

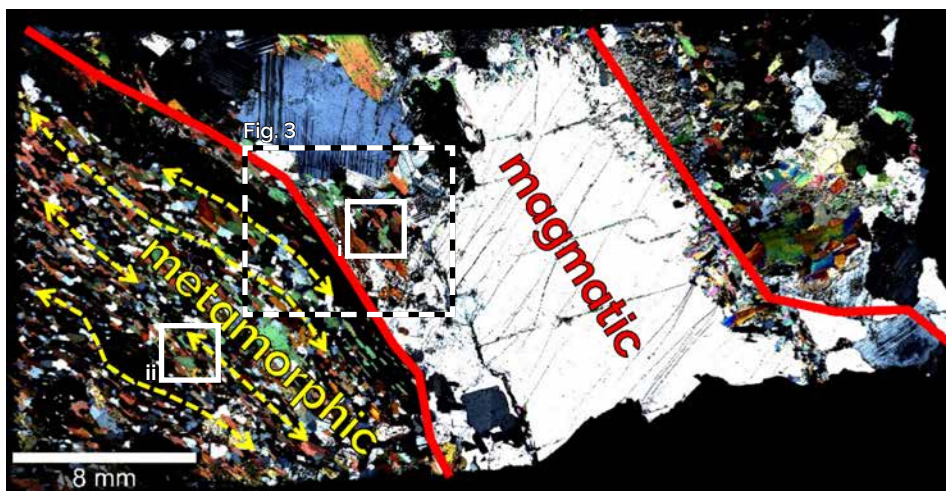


Figure 2: Overview white light image of metamorphic rock with magmatic domain.

Cross-polarization illumination showing a magmatic vein (red) crosscutting a metamorphic rock along its pre-developed metamorphic fabric (yellow). White rectangles (i and ii) represent the selected areas for the following measurements; position of Figure 3 indicated with box.

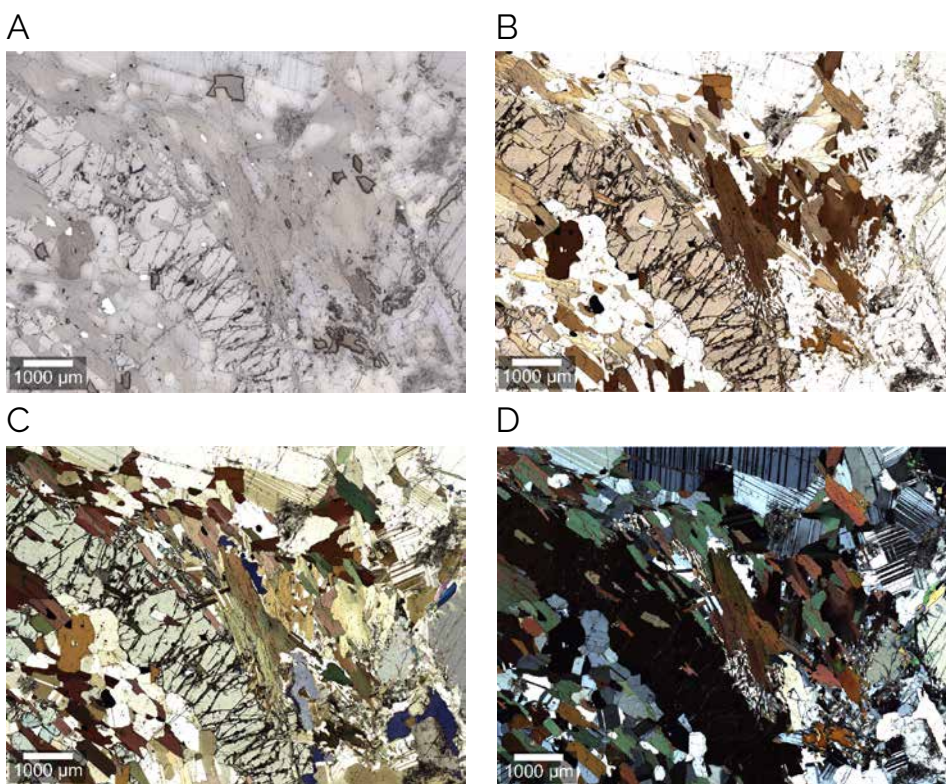


Figure 3: White light images of biotite mineral acquired using different illumination techniques.

Reflected (A) and transmitted (B) light image. Transmitted light image at parallel polarization ($\parallel\text{Pol}$) (C) and 90° crossed polarization setup (xPol) (D). Area section given in Figure 2.

Polarization-resolved Raman spectroscopy of biotite

Raman spectroscopy was employed to test our hypothesis on the origin of two biotite generations in the rock. The first approach was a statistical investigation of two areas in the sample (respectively Figure 2: white squares) that recorded fully automated 360° polarizer series on 15 randomly selected biotite crystals in

both areas. A 50x/0.8NA objective and a 532 nm excitation laser at 10 mW were used. A series of single spectra was acquired at an integration time of 0.5 s per spectrum and 10 accumulations with a polarizer angle step size of 5° through a full rotation. Two selected Raman modes of biotite and schematic representations of their respective vibrations in the crystal structure are given in Figure 4. Both the

νTO_4 stretching mode (T-O stretch of SiO_4^- and AlO_4^- -tetrahedron movements along the c-axis, green vectors) and the $\delta\text{T}_6\text{O}_6$ ring modes (O3-T-O1 and T-O2-T bend in the T_6O_6 -ring adjacent to the cleavage planes, blue vectors) were pre-evaluated to be unaffected by birefringence effects (Figure 4B) [3,4].

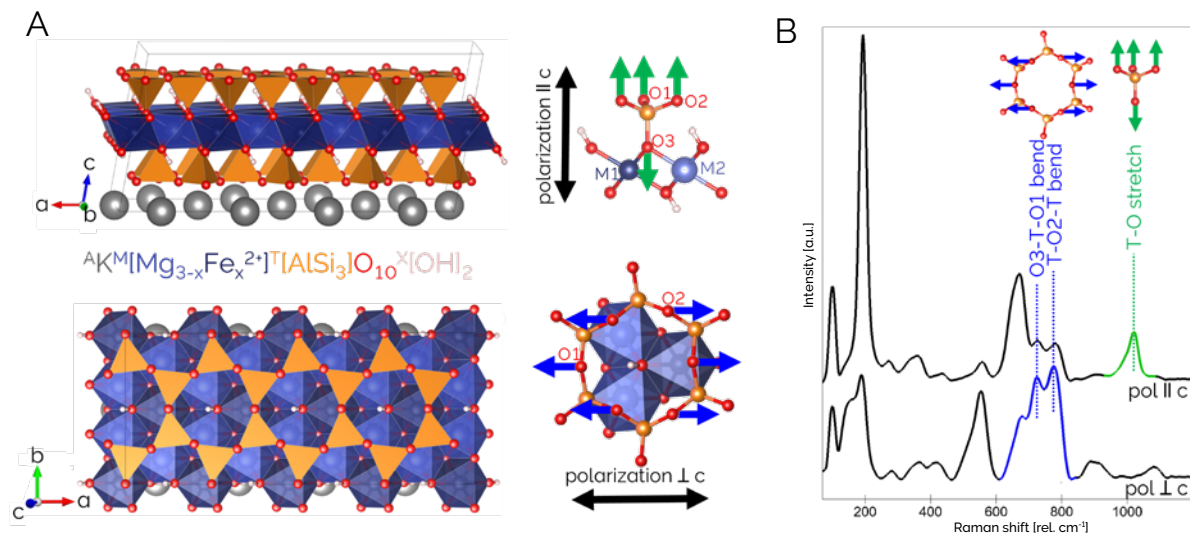


Figure 4: Structural formula, crystallographic models and polarization-resolved Raman spectra of biotite.

(A) Crystallographic models parallel to the b- and c-axis and structural formula of biotite. Coupling relationships are given for polarization orientations parallel and orthogonal to the c-axis. (B) Resulting polarization-dependent Raman spectra which exaggerate T-O stretch parallel to c-axis (SiO_4^- and AlO_4^- -tetrahedron) and O3-T-O1 and T-O2-T bend orthogonal to c-axis (T_6O_6 -ring).

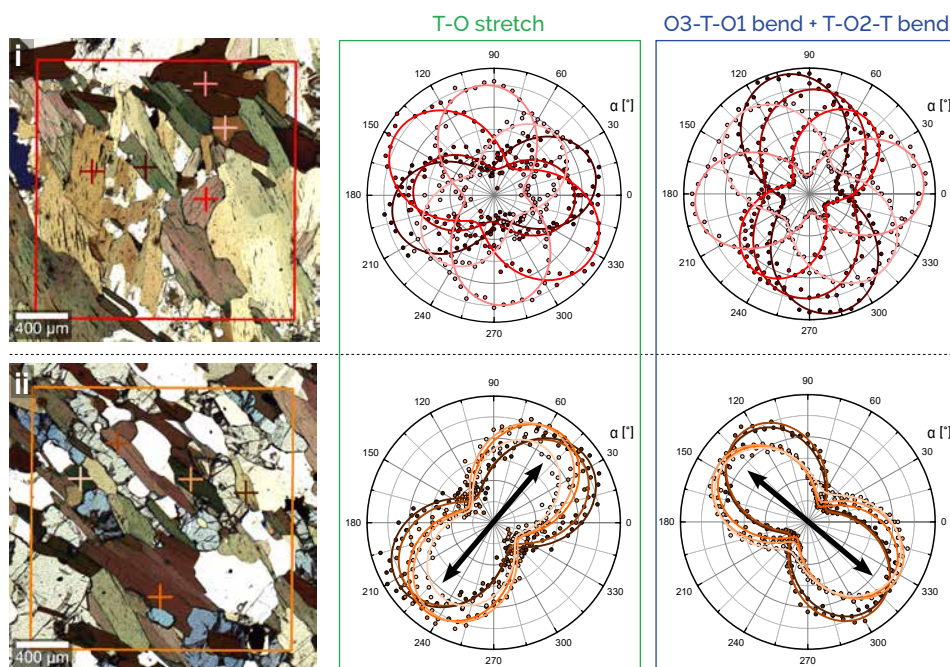


Figure 5: Polar plots of the biotite crystal orientations.

Measurement points and polar orientation plots of 5/15 polarizer series from the magmatic (i) and metamorphic region (ii).

For evaluation, polar orientation plots were extracted displaying the Raman band intensities of the νTO_4 stretching mode (green) and $\delta\text{T}_6\text{O}_6$ ring modes (blue) (Figure 5, 5 positions per area plotted). In the metamorphic part (ii) a clear orientation of the TO_4 -tetrahedrons' T-O stretching mode along the 45° and 225° polarizer rotation and thus parallel to the former maximum pressure-induced stress regime can be observed. The O3-T-O1 and T-O2-T bending vibrations of the T_6O_6 -rings, which correspond to the anisotropy of the crystal lattice and the preferred orientation of the layered structure of the biotite parallel to the (001) surface, are statistically regulated along the 135° and 315° polarization. In the magmatic part (i), however, the crystal axes are irregularly oriented in all spatial directions.

TrueComponent Analysis of biotite in Raman images

In a second approach, high-resolution confocal Raman images were acquired from the magmatic (i) and metamorphic (ii) areas and analyzed using the WITec TrueComponent Analysis data evaluation module. The images were recorded in a $2000 \times 2000 \mu\text{m}^2$ area at 0.1 s integration time per spectrum using a 50x/0.8 NA objective and a 532 nm excitation laser at 40 mW. In this analysis setup, only biotite spectra were included and three orientation endmembers (blue, green and red; Figure 6A: selected endmember crystals, Figure 6D: endmember Raman spectra) were pre-defined as internal standards for the crystallographic orientations. Their allocation was based on a detailed evaluation of the phase identification and by the determination of their crystallographic axis orientation in xPol illumination.

As a result, the TrueComponent Analysis algorithm created intensity distribution images (Figure 6B) in which the coloring of individual grains represents their orientation match with the pre-defined endmember orientations. The color palettes (inverse pole figures: red, blue and green) therefore correspond to spatial orientations in which the excitation laser is aligned perpendicular to the biotite (100), (010) and (001) sectional planes and the laser polarization is aligned in parallel with the crystallographic c-, a- and b-axes, respectively (Figure 6C).

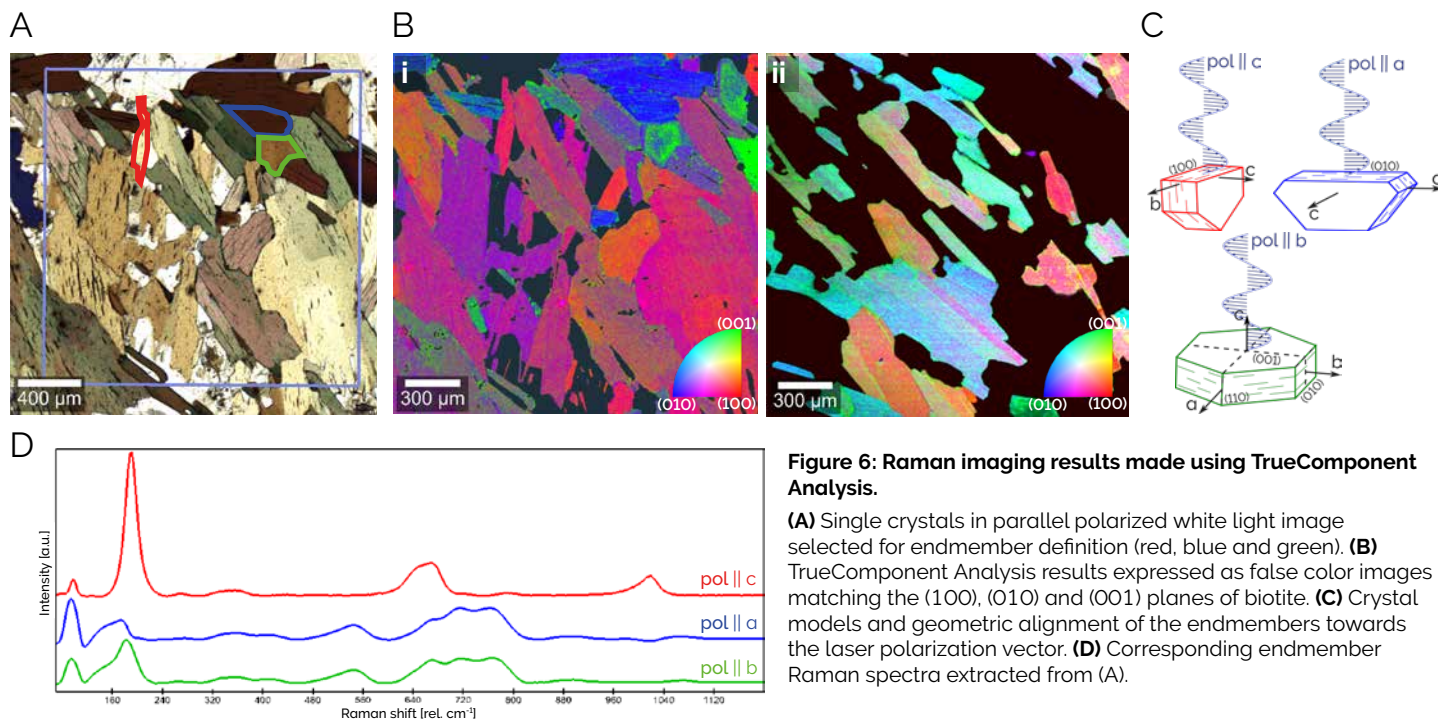
The colors in the magmatically formed area (i) are close to the extremes of the color scale, indicating arbitrary biotite orientations in this section that originate from random crystallization in a melt phase. In contrast, the image of metamorphically regulated biotites (ii) shows a more uniform color spectrum, pointing to a similar orientation of all biotites in this area having been caused

by high pressures applied over a long period of time.

In combination with the statistical Raman spectroscopic approach, these results confirm a difference in the two parts of the thin section with highly ordered biotite crystals in the metamorphic and irregular orientations in the melt emplacement areas, supporting the hypothesized manner of formation.

Conclusion

This study presented polarized white light and polarization-resolved Raman microscopy as effective methods for investigating biotite crystals and their crystallographic orientation. Using semiquantitative approaches, the data supported the hypothesis of different crystallization stages in the rock formation. This clearly demonstrates the benefits of both techniques for characterizing geoscience samples.



References

- [1] Nicol, W. (1829). On a method of so far increasing the divergency of the two rays in calcareous-spar, that only one image may be seen at a time. *Edinburgh new philosophical journal*, 6, 83-84.
- [2] Amici, G. B. (1844). Note sur un appareil de polarisation. *Ann. Chim. Phys.*, 12, 114-120
- [3] McKeown, D. A., Bell, M. I., & Etz, E. S. (1999). Raman spectra and vibrational analysis of the trioctahedral mica phlogopite. *American Mineralogist*, 84(5-6), 970-976. DOI: 10.2138/am-1999-5-634.
- [4] Aspiotis, S., Schlüter, J., Redhammer, G. J., & Mihailova, B. (2022). Non-destructive determination of the biotite crystal chemistry using Raman spectroscopy: how far we can go?. *European Journal of Mineralogy*, 34(6), 573-590. DOI: 10.5194/ejm-34-573-2022

Info Box: Polarization-resolved Raman spectroscopy

Raman spectroscopy that makes use of polarization effects relies on the electromagnetic nature of light, as polarization corresponds to the direction along which the electric field is oscillating. The wave equation (derived from Maxwell's equations) dictates that the magnetic and electric fields of the electromagnetic wave always oscillate perpendicular to its propagation direction.

While unpolarized light is a superposition of waves with their electric fields oscillating in random directions, the electric fields of all waves are oriented in parallel for polarized light. Dependent on the molecular symmetry of the sample,

the vibrational modes visible in the Raman spectra can be sensitive to the polarization angle of the excitation light. This reflects in a vibrational mode's Raman signal strength varying with the angle of polarization of the incident light, as visible in many in-plane anisotropic samples.

At the same time, unoriented or isotropic crystal/molecular structures show no pronounced polarization dependence in their individual Raman peak intensities. Consequently, polarization-resolved Raman spectroscopy can provide much more profound information on the studied sample such as its structure and orientation of different domains.

WITec Microscopes



alpha300 S:
Scanning Near-field
Optical Microscope

alpha300 A:
Atomic Force
Microscope

alpha300 Ri:
Inverted Confocal
Raman Microscope

RISE®: Raman Imaging
and Scanning Electron
Microscope

alpha300 apyron™: Automated
Confocal Raman Microscope

alpha300 R: Confocal
Raman Microscope

alpha300 access:
Confocal Micro-Raman System

Find your regional WITec and Oxford Instruments contact at <https://raman.oxinst.com/contact>

WITec Headquarters

WITec Wissenschaftliche Instrumente und Technologie GmbH
Lise-Meitner-Str. 6, D-89081 Ulm, Germany
Phone +49 (0) 731 140 700, Fax +49 (0) 731 14070 200
info@witec.de, <https://raman.oxinst.com>